

See discussions, stats, and author profiles for this publication at: <https://www.researchgate.net/publication/231650272>

Influence of the Side Group Aromaticity on the Organic Molecule Adsorption on Cu(110)

ARTICLE *in* THE JOURNAL OF PHYSICAL CHEMISTRY C · JULY 2008

Impact Factor: 4.77 · DOI: 10.1021/jp8037297

CITATIONS

8

READS

10

2 AUTHORS, INCLUDING:



E. Rauls

Universität Paderborn

116 PUBLICATIONS 1,973 CITATIONS

SEE PROFILE

Influence of the Side Group Aromaticity on the Organic Molecule Adsorption on Cu(110)

E. Rauls* and W. G. Schmidt

Lehrstuhl für Theoretische Physik, Universität Paderborn, 33095 Paderborn, Germany

Received: April 29, 2008; Revised Manuscript Received: May 28, 2008

Density functional theory (DFT) is used to analyze in detail the adsorption of $\text{C}_4\text{H}_9\text{NO}_2$ (gaba), $\text{C}_9\text{H}_{17}\text{NO}_2$ (gabapentin) and $\text{C}_9\text{H}_{12}\text{NO}_2$ on the (110) surface of Cu. The adsorption configurations are found to be similar to those of phenylglycine. Like the latter, both molecules bind via the oxygen atoms and the nitrogen atom to the surface metal atoms. The stability of the adsorbate system, however, depends substantially on the remaining part of the molecule, among others whether a side group is attached and whether it is an aromatic (phenylgroup) or a nonaromatic (cyclohexyl) ring. The pure intermolecular interaction, depending on the adsorbate density, has been compared to the adsorbate–substrate interaction, showing that the latter is the main stabilizing factor for both systems. Considering long-range dispersive forces—neglected in DFT—leads to a substantial further stabilization of the adsorbates.

I. Introduction

The adsorption of organic molecules on metal surfaces is currently intensively investigated, both for reasons of scientific curiosity as well as technological importance.^{1,2} Following the ideas of a bottom-up approach, self-organization of organic molecules on metal surfaces appears as one of the most promising approaches to the further miniaturization of electronic devices.^{3–7} Organic molecules with different features offer as building blocks numerous possibilities to form one-, two-, or three-dimensional networks. Some systematic overview can be gained upon investigating these network formation possibilities depending on both the directly (like e.g. H-bond donation) and indirectly (like, e.g., steric hindrance) contributing functional parts of a molecule. For this aim, an atomistic understanding of the interaction of single molecules with a substrate is one of the first steps.^{8–10} Several groups have tried to understand the character of adsorption of organic molecules on copper surfaces in detail by carrying out first principles and other calculations. One example that also is of pharmaceutical importance is tartaric acid, being one of the few molecules for which heterogeneous catalytic reactions with practically relevant enantiomeric excess could be realized by chiral modification of an otherwise nonchiral metal surface.^{11,12} A similar example are the investigations of methyl pyruvate on chirally modified platinum surfaces.^{5,13}

In this work, we focused on the investigation of the adsorption of the 2-[1-(aminomethyl)cyclohexyl]acetic acid ($\text{C}_9\text{H}_{17}\text{NO}_2$) molecule on a copper (110) surface. This molecule is an amino acid that is commonly known from pharmacology under the generic name *Gabapentin*. Initially, it was synthesized to mimic the chemical structure of the neurotransmitter γ -aminobutyric acid ($\text{C}_4\text{H}_9\text{NO}_2$, gaba) by addition of a cyclohexyl group to the backbone of this molecule. It is used as an anticonvulsant to treat epileptic seizures, amyotrophic lateral sclerosis (ALS), and painful neuropathies.^{14,15} Gabapentin interacts with a high-affinity binding site in brain membranes, which has recently been identified as an auxiliary subunit of voltage-sensitive Ca^{2+} channels in the central nervous system.^{16,17} Like this, its mechanism of action is known to differ from those of other

anticonvulsant drugs. Nevertheless, especially in the operational area of neuropathic pain, its mechanisms of action are not yet fully understood.

An investigation of this molecule and its interaction with other biological molecules involved in aforementioned processes, like, e.g., amino acids, as well as an investigation of how optional side groups affect the properties of the molecule can therefore not only have implications for device technology but also for pharmaceutical questions and applications, not at last in the search for drugs with reduced adverse reactions.

A copper surface has been chosen for our first investigations of the system, since this surface is known to be highly reactive compared to other coin metals.¹⁰ To our knowledge, so far no experimental investigations exist on such a system, but for practical reasons the copper surface might well be among the first surfaces to be studied in this context. Furthermore, this surface allows us to compare our results to those obtained for similar molecules,²³ which had been stimulated by scanning tunneling microscopic experiments.¹⁸

The following section briefly describes the computational setup we used. In the third section, we present and discuss the results of our calculations. A summary rounds off the article in section IV.

II. Computational Details

We have performed first principles density functional calculations with the Vienna ab initio Simulation Package (VASP).²⁰ The electronic interactions are described by the projector-augmented wave (PAW) method,²⁰ which allows for an accurate treatment of the first row elements as well as the Cu 3d electrons with a relatively moderate energy cutoff. A value of 340 eV for the energy cutoff together with a $(1 \times 2 \times 1)$ Monkhorst–Pack k -point sampling has been used for all calculations throughout this work. The PW91 functional is used to model the electron exchange and correlation (XC) effects within the generalized gradient approximation (GGA).²¹ The modeling setup is, thus, comparable to that used in ref 12, where also the same method has been used to model tartaric acid molecules on Cu(110).

The surface slabs were modeled with six layers of metal atoms and a vacuum region corresponding to 12 layers. The lowest layer of surface atoms was kept fixed, while all other atoms

* Corresponding author.

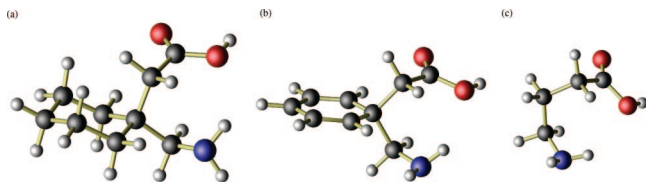


Figure 1. Geometry of the most stable conformer of (a) the gabapentin molecule (GP), (b) the gabapentin molecule with an aromatic phenyl-group instead (AGP), and (c) the gaba molecule.

were allowed to relax freely. In particular for the comparison of the electrostatic interaction between the adsorbed molecules, we have performed calculations for different molecular densities along the (110) direction. Therefore, results are shown for supercells with a lateral extension of (4×3) and (4×6) copper unit cells.

Long range dispersive interactions have been investigated in additional calculations, where the long-range dispersive forces (vdW), which are not included in DFT, have been added to the electron xc modeled in GGA. This procedure rests on a semiempirical modeling of vdW effects via Londons dispersion formula and has been outlined in detail and tested for various systems in refs 10 and 23.

III. Results and Discussion

The atomistic structure of the gabapentin (GP) molecule is similar to that of phenylglycine: a 6-fold carbon ring functionalized by a carboxyl group and an amine group are the main constituents of both molecules. In GP, however, both the carboxyl and the amine group are connected via a CH_2 group to one of the carbon atoms of the ring. Furthermore, the ring in the GP molecule is not aromatic but saturated with five additional hydrogen atoms. The geometry of the most stable conformer of GP is shown in Figure 1a. In order to compare our results to previous results for phenylglycine²³ on the one hand, and on the other hand to filter out the influence of the ring being an aromatic or not, we calculated another molecule, in which five hydrogen atoms of the cyclohexyl group have been removed from the carbon ring, thus making it an aromatic phenylgroup. The geometry of this molecule, $\text{C}_9\text{H}_{12}\text{NO}_2$ (in the following abbreviated as AGP), is shown in Figure 1b. The geometry of the neurotransmitter gaba with the sum formula $\text{C}_4\text{H}_9\text{NO}_2$ is shown in Figure 1c. In this molecule, the carbon ring is removed, so that only three CH_2 groups remain to connect the amine and the carboxyl group.

Many findings concerning the bonding mechanism of the GP and AGP molecules correspond to those of phenylglycine (PGL) and shall, therefore, not be repeated here. For details, the interested reader is referred to ref 24. Both GP and AGP can chemisorb on the surface with only the amine group and the double bonded oxygen binding to Cu atoms, while no bond is formed between the OH-group and the surface. These structures have, though, only a small binding energy of approximately 0.14 eV, and analogous to the case of PGL, molecular adsorption is favored for those species of the molecules, in which the oxygen atom is deprotonated and the H atom leaves in form of H_2 from the structure. From experiments it is known that the respective hydrogen atom is mobile on the Cu surface at rather low temperatures and desorbs at room temperature,^{24,25} such that it does not need to be considered in our calculations. Also in this treatment, we proceed similar as Hermse et al. in ref 12.

Like in case of PGL, the (O-deprotonated) GP prefers an adsorption configuration in which the nitrogen atom of the amine group binds to a Cu atom of a close packed (110) row of the

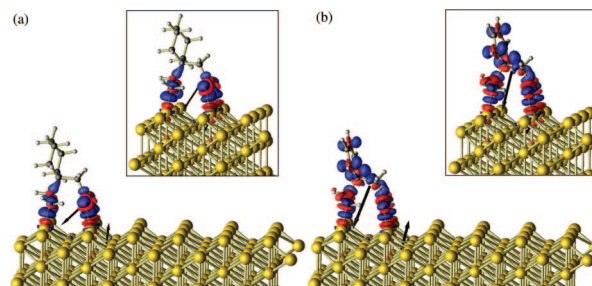


Figure 2. Induced charges and dipoles between the substrate and (a) the GP-molecule or (b) the AGP-molecule, respectively. Blue areas mean electron accumulation, red areas depletion. Both the small cell and the cell doubled along the (110) direction are shown. For all structures, an isovalue of ± 0.02 has been chosen. The vectors have been attached to the calculated positions of the induced dipoles.

TABLE 1: Comparison of the bond lengths and angles of GP, AGP, and gaba^a

	bond lengths			angles			
	N—Cu	O1—Cu	O2—Cu	N	O1	O2	CO ₂
GP	2.08	1.98	2.00	112	125	118	12
AGP	2.07	2.02	2.01	114	126	118	10
gaba	2.09	1.98	2.00	116	124	120	8

^a Labeling corresponds to Figure 3. All lengths in Å and angles in deg.

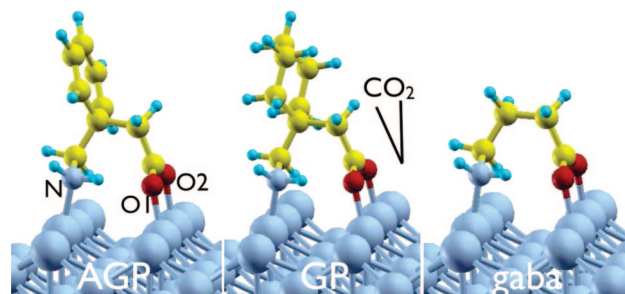


Figure 3. Adsorption geometries of the three molecules on the surface after deprotonation of the O1 atom.

substrate and the oxygen atoms bind to Cu atoms of an adjacent close packed row, compare Figure 2a. In analogue, Figure 2b shows the most stable adsorption configuration for AGP.

Table 1 summarizes the calculated bond lengths (columns 1–3) and bond angles (columns 4–7) for the adsorbate structures. The labeling refers to Figure 3. The calculated bond lengths are 2.08 Å for the N—Cu bond, and 1.98 and 2.00 Å for the two O—Cu bonds in case of GP. For AGP, the respective values are 2.07, 2.02, and 2.01 Å, and for gaba, they are 2.09, 1.98, and 2.00 Å. The only small deviations of these values from each other as well as from the results for PGL indicate the mainly local character of the bonding, or equivalently the small influence of the exact nature of the nonbonding parts of the adsorbate.

The bonding angles around the nitrogen and the two oxygen atoms are 112°, 125°, and 118° for GP and 114°, 126°, and 118° for AGP, respectively. For the gaba molecule, angles of 116°, 124°, and 120° are found. Due to the additional CH_2 -group compared to PGL, the CO_2 -group is in GP, AGP and gaba oriented much closer to the surface normal, i.e., 12°, 10°, and 8°. At the same time, the cyclohexyl group of GP and the phenylgroup of AGP are slightly stronger tilted away from the surface normal, namely 12° and 17° compared to 9° in case of PGL, which, however, might be an enlarged value due to the high adsorbate density. Some deviations can be explained due

to the smaller supercells used in ref 24, where the experimental observations suggested the use of a (2×3) cell. The density of molecules in the adstructure is twice as high as in this work, and the molecular separation in the adstructure is considerably smaller. Higher binding energies and steeper geometries can therefore be expected for this system.

Upon adsorption of the molecules, not only the molecule is deformed, but also the Cu atoms involved in the bonding are lifted out of the surface plane. In case of GP, the Cu atom that forms the bond to the amine group is lifted up by 0.14 Å, the two Cu atoms below the oxygen atoms of the molecule are elevated by 0.12 Å and 0.10 Å, respectively. For AGP, the nitrogen atom pulls the underlying Cu atom by 0.17 Å out of the surface plane, the Cu atoms below the two oxygen atoms are by 0.06 and 0.08 Å less strongly moved from their original positions. The same values as for AGP are found for gaba. The only slight variations of these geometrical quantities suggests that neither the phenyl group of AGP nor the cyclohexyl group of GP have an essential influence on the bonding to the substrate.

Differences occur, however, in the energetics. The adsorption energy of the (O-deprotonated) molecules on the surface can be calculated as

$$E_{ad} = E_{mollsurf} - E_{surf} - E_{mol} + \frac{1}{2}E_{H_2} \quad (1)$$

under consideration of hydrogen desorption from the surface as H_2 molecules and with the energies of the relaxed Cu(110)-surface and molecules as reference values. In the equation, the first term denotes the total energy calculated for the surface with the molecule chemisorbed. The second and third term denote the total energies of the free (and relaxed) surface and molecule, respectively. Note that the molecule is in its ground-state and still contains the hydrogen atom at the oxygen atom, which is first lost upon adsorption. To correct for this, the last term accounts for the energy of the additional hydrogen atom (compare ref.). For GP, calculations yield $E_{ad} = -0.92$ eV; for AGP this value is $E_{ad} = -0.93$ eV. For the pure gaba molecule, an adsorption energy of $E_{ad} = -0.97$ eV has been calculated.

Although, like in case of PGI, three bonds to the substrate are formed, this is a rather small value, which is, furthermore, considerably smaller than the comparable value for PGI ($E_{ad} = -1.35$ eV).²³ This value might, however, be enlarged by a stabilization within the adsorbate.

As a second contribution to the total chemical bonding energy, we have calculated the energies due to the deformation of both the molecule and the surface upon adsorption. For PGI, a value of 2.75 eV had been obtained²³ for this strain contribution, adding up with E_{ad} to a total bonding energy of -4.10 eV. For the adsorption of GP on the Cu(110) surface, the molecule is deformed with 0.37 eV, the surface with 0.88 eV, giving a total strain energy of 1.25 eV. A slightly higher value is obtained for AGP, where the molecular deformation energy is 0.56 eV, the deformation energy of the surface is 0.86 eV, resulting in a total strain energy of 1.42 eV. For the adsorption of gaba, the surface has to be deformed with 0.84 eV, the molecule with 0.37 eV, giving a total strain energy of 1.21 eV for this molecule. Summing these two contributions to the chemical bonding energy up for all three molecules, we obtain $E_{bond} = -2.16$ eV for GP, $E_{bond} = -2.35$ eV for AGP, and $E_{bond} = -2.19$ eV for gaba. In spite of its much simpler structure, gaba exhibits an adsorption behavior very similar to GP. This indicates that the bonding part of the molecule is merely unaffected by the presence of the nonaromatic cyclohexyl group of GP. The phenyl group of AGP, in contrast, leads to larger differences.

TABLE 2: Comparison of the adsorption energies of GP, AGP, and gaba in the two different cells^a

	DFT		DFT+vdW	
	(4 × 3)	(4 × 6)	(4 × 3)	(4 × 6)
GP	0.92	1.46	2.98	2.73
AGP	0.93	1.47	2.84	2.58
gaba	0.97	1.51	2.68	2.44

^a The first two columns show the pure DFT results; the last two columns show the calculations with additional vdW interactions. All values in eV.

A stronger deformation of the molecule makes bonding slightly stronger than for the gaba molecule without a further side group or for GP with its nonaromatic cyclohexyl group. However, both a stronger deformation of the constituents and a larger adsorption energy in case of phenylglycine lead to a 75% higher bonding energy compared to AGP, but especially the higher strain energy might be due to the twice as high molecular density in the adstructure. We focus, however, on the adsorption of one molecule rather than an ordered adstructure, and therefore turned to the investigation of a system with an even larger molecular separation. If we double the cell along the (110) direction and calculate the adsorption energies for this cell, we obtain $E_{ad} = -1.46$ eV for GP, $E_{ad} = -1.47$ eV for AGP, and $E_{ad} = -1.51$ eV for gaba. The energy difference is, thus, the same, namely a stabilization of 0.54 eV for all three molecules. Hence, the special form of the restgroup does not lead to different interactions across the supercell boundaries. Table 2 summarizes the calculated adsorption energies (first two columns).

Whether the side group has an influence on the electrostatics of the system can be investigated by analyzing the charge transfer between substrate and chemisorbed molecules. Dividing the system into two parts, namely surface and adsorbate, by planes located at the position of maximum local charge transfer along the bonds formed between these two subsystems, the individual contributions to the electrostatic interaction energy can be calculated. This mechanism has been described previously in refs 10 and 23.

A net charge transfer is found to occur, like in case of PGI, from the metal surface toward the chemisorbed molecules. For GP, 0.14 electrons are transferred (in the small cell), for gaba 0.15 electrons, i.e. slightly less than for PGI (0.16 e). For AGP, the charge transfer is with 0.20 electrons slightly larger. The calculated dipoles that are located in the substrate region and in the adsorbate region are found to be considerably stronger for AGP than for GP or gaba. In case of AGP, these two dipoles have the strengths of 10.1 D (substrate) and 15.0 D (adsorbate), while the respective dipole strengths are only 7.7 D for both substrate and adsorbate in case of GP. For gaba, dipoles of 8.13 D (substrate) and 8.19 D (adsorbate) are found. The effect of the stronger dipoles for AGP is, however, compensated in part by the larger distance between these dipoles compared to GP. This is indicated by the black arrows in Figure 2. The vectors have been attached to the calculated positions of the induced dipoles. In GP, the dipole in the adsorbate region is located close to the carboxyl carbon atom. Due to the aromatic phenylgroup of AGP, the dipole induced in the adsorbate region for this molecule is located further away from the surface, such that the dipole-dipole distance becomes ≈ 1.3 Å larger than for GP. The directions of the dipoles are the same for both molecules, i.e., with the surface dipole pointing outward the surface and the molecular dipole slightly slanted toward the surface. In the expression

$$E_{\text{static}} = E_{\text{dip/dip}} + E_{\text{mon/mon}} + E_{\text{mon/dip}} + E_{\text{dip/mon}} \quad (2)$$

for the total electrostatic energy, the dipole–dipole interaction turns out to be the essential term. A weak attractive Coulomb interaction of ≈ 0.1 eV is found for GP and AGP as well as for PGI. The strongest contribution, however, the dipole–dipole interaction, is repulsive, thus resulting in total in a repulsive electrostatic interaction energy of 0.40 eV for GP, 0.47 eV for gaba, and 0.56 eV for AGP, compared to 0.36 eV for PGI.²³

The obtained values are small compared to the total adsorption energy and are, hence, not the determining contributions. The conclusion that the bonding character of both molecules to the substrate is, like for PGI, essentially covalent, is underlined by the visualization of the induced charge density as shown in Figure 2. Isosurfaces are plotted for ± 0.02 e in parts a and b. Electron accumulation occurs in the blue areas, i.e. along all three N–Cu and O–Cu bonds to the substrate.

For the enlarged cell, the charge transfer is calculated to 0.15 e (0.18 e) for GP (AGP). The surface dipole of GP is slightly reduced in the doubled cell (7.6 D), while the molecular dipole is increased (9.7 D). In case of AGP, both the surface and the molecular dipole are decreased to 8.6 and 13.5 D, respectively. The total electrostatic energy is reduced to 0.14 eV for GP and 0.10 eV for AGP, showing that this interaction in the small cell to a large extent has to be ascribed to an intermolecular interaction across cell boundaries. This strong reduction of the repulsive electrostatic interaction at larger molecular separation explains to a great deal the stabilization expressed in the overall adsorption energies.

For both the (4×3) and the (4×6) cell, additional calculations have been made that include the long-range dispersive interactions. For the small cell, we find a drastic increase in the adsorption energies, i.e. $\Delta E_{\text{ad}} = 2.06$ eV for GP, $\Delta E_{\text{ad}} = 1.91$ eV for AGP, and $\Delta E_{\text{ad}} = 1.71$ eV for gaba. For the bigger cell, the adsorption energies are, similarly, found to increase, but only by $\Delta E_{\text{ad}} = 1.27$ eV for GP and $\Delta E_{\text{ad}} = 1.11$ eV for AGP, and $\Delta E_{\text{ad}} = 0.93$ eV for gaba, respectively. Consequently, the adsorption energies in the systems with larger molecular separation are decreased by 0.25 (0.26, 0.24) eV for GP (AGP, gaba), compare Table 2. We, thus, have two competing effects of DFT and dispersive interactions: while DFT suggests a stabilization upon lowering the adsorbate density, calculations including dispersive interactions predict the opposite, although less pronounced. This means that the inclusion of the vdW interaction does not only stabilize the structures but also leads to qualitatively different results. First, the differences between the adsorption energies of the three different molecules is with 0.30 eV larger than for pure DFT (0.05 eV). Second, the intermolecular interaction of the adsorbate becomes less important. The variation of the adsorption energies with the molecule spacing is reduced and the effect reversed in favor of a higher adsorbate density, as calculations with different supercells have shown. However, when discussing these results, a word of caution is in order: the contribution of long-range dispersive interaction is modeled here using a sum of pairwise contributions calculated from the atomic polarizabilities and ionization energies vs the London dispersion formula.²² This procedure can be expected to yield estimates for the size of the effects related to dispersion interactions but no quantitative predictions, in particular for metallic systems.

In order to find out how much the pure intermolecular interaction contributes to this effect, we have investigated the adstructure separately from the substrate. Figure 4 shows how the inclusion of the long-range dispersive interaction affects the total energy of the gas phase molecules (i.e., deprotonated as

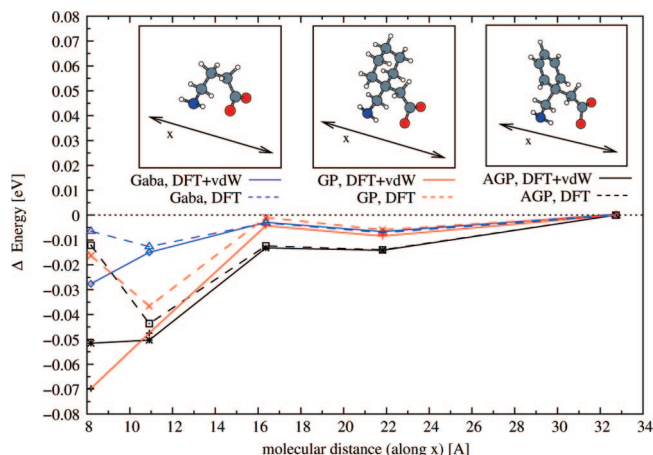


Figure 4. Distance dependent energy differences for the molecules GP (red), gaba (blue), and AGP (black) in the gas phase. Pure DFT calculations (dashed lines) in comparison to DFT calculations including an additional London dispersion term (solid lines). The size of the supercell has been varied along the x -axis, i.e., perpendicular to the plane of the carbon ring.

in the adsorbate). The size of the supercell has been varied along the x -axis, i.e. perpendicular to the plane of the carbon ring, and the molecules. If the molecules in the gas phase, were relaxed, they would, of course, depending on their distances, reorient and deform (e.g., rotation of the carboxyl group). This would not give us the desired information, and therefore, we kept the molecules fixed in their respective adsorption positions. For distances larger than 16 Å, the inclusion of vdW interactions shows only a weak effect. AGP is stabilized more strongly (< 0.02 eV/molecule) than GP (< 0.01 eV/molecule). For smaller distances, the effect becomes larger. For a distance of 11 Å, both molecules are stabilized by about 0.05 eV, with a vdW contribution of 0.011 eV (0.007 eV) in case of GP (AGP). For smaller distances, the repulsive part of the interaction becomes larger. In the pure DFT calculations, the system gets destabilized again. However, vdW interactions can make up for this and lead to a further stabilization, in particular for GP (0.07 eV/molecule at 8 Å distance.). The gaba molecule shows, qualitatively, a very similar behavior to GP. As could be expected, intermolecular interaction is much smaller for this molecule. At a distance of 11 Å, the stabilization amounts only to 0.015 eV, and the additional dispersive interaction has nearly no influence. For a separation of 8 Å, the stabilization due to vdW interactions becomes stronger, ≈ 0.03 eV, while it is below 0.01 eV for pure DFT. An important result of these comparative calculations is the qualitative difference resulting from the various energetic contributions, leading to an energetic minimum for all three molecules in case of the pure DFT calculations, but not (or at a different distance) if the dispersive interactions are included. This shows that the consideration of such long-range terms can also be important if dealing with shorter range problems, in particular, if aromatic molecules are involved. Nevertheless, comparing these numbers with the energy differences discussed above, we can conclude that the main part of the stabilization has to originate from the molecule–substrate interaction. The difference in the adsorption energies of the molecules in the smaller cell (≈ 11 Å distance) and the bigger cell (≈ 22 Å distance) of about 0.7 eV is an order of magnitude larger than what we can explain from the pure molecular interactions.

IV. Conclusions

In summary, we have shown that GP, AGP, and gaba show an adsorption behavior on copper comparable to that of phenylglycine. In both cases, bonding is covalent, and adsorption is stabilized by a strong deformation of both the surface and the molecule. The larger contribution to the molecular strain energy is found for AGP, in which the aromatic phenylgroup represents a smaller steric hindrance than the cyclohexyl group of GP. Nevertheless, both the adsorption energy and the strain energy are considerably smaller than for phenylglycine. At least part of the difference might be due to the higher adsorbate density in case of PGI. Comparing our GP and AGP calculations with those of PGI and gaba, we find that apparently not electronic/electrostatic effects but rather the presence of an additional CH₂ group, which determines the bonding angle of the carboxyl group, affects the energetics of adsorption. The presence of an aromatic side group enhances the molecular polarizability, but is, nevertheless, of local character and does not change the bonding characteristics compared to the molecule with the nonaromatic side group. Calculations including long-range dispersive interactions show that these contribute essentially to the stability of the system and also lead to qualitative changes. Comparisons with gas phase calculations show that the molecule-substrate interaction is the determining quantity, while the pure intermolecular interaction plays a minor role and can not account for the qualitative differences between pure DFT and vdW calculations.

Acknowledgment. Calculations were performed at the Pad-erborn Center for Parallel Computing (PC²) and the Höchstleistungs-Rechenzentrum Stuttgart. E.R. would like to thank Dr. T. Schaten for drawing her attention to the gabapentin molecule.

References and Notes

- (1) Nilsson, A.; Pettersson, L. G. M. *Surf. Sci. Rep.* **2004**, *55*, 49.

- (2) Schmidt, W. G.; Seino, K.; Preuss, M.; Hermann, A.; Ortmann, F.; Bechstedt, F. *Appl. Phys. A: Mater. Sci. Process.* **2006**, *85*, 387.
- (3) Schnadt, J.; Rauls, E.; Xu, W.; Vang, R. T.; Knudsen, J.; Laegsgaard, E.; Li, Z.; Hammer, B.; Besenbacher, F. *Phys. Rev. Lett.* **2008**, *100*, 046103.
- (4) Xu, W.; Dong, M.; Gersen, H.; Rauls, E.; Vazquez-, Campos, S.; Crego-Calama, M.; Reinhoudt, D. N.; Stensgaard, I.; Laegsgaard, E.; Linderoth, T. R.; Besenbacher, F. *Small* **2007**, *3*, 854.
- (5) Rauls, E.; Hammer, B. *Catal. Lett.* **2006**, *106*, 111.
- (6) Mamdoui, W.; Dong, M.; Xu, S.; Rauls, E.; Besenbacher, F. *J. Am. Chem. Soc.* **2006**, *128*, 133057 pages.
- (7) Xu, S.; Dong, M.; Rauls, E.; Otero, R.; Linderoth, T. R.; Besenbacher, F. *Nano Lett.* **2006**, *6*, 1434.
- (8) Weigelt, S.; Busse, C.; Petersen, L.; Rauls, E.; Hammer, B.; Gothelf, K. V.; Besenbacher, F.; Linderoth, T. R. *Nat. Mater.* **2006**, *5*, 112.
- (9) Preuss, M.; Schmidt, W. G.; Bechstedt, F. *Phys. Rev. Lett.* **2005**, *94*, 236102.
- (10) Rauls, E.; Blankenburg, S.; Schmidt, W. G. *Phys. Rev. B* **2008**.
- (11) Barbarosa, L. A. M. M.; Sautet, P. *J. Am. Chem. Soc.* **2001**, *123*, 6639.
- (12) Hermse, C. G. M.; van Bavel, A. P.; Barbosa, A. P. J.; Sautet, P.; van Santen, R. A. *J. Phys. Chem. B* **2004**, *108*, 11035.
- (13) Vargas, A.; Burgi, Th.; Baiker, A., J. *Catal.* **2004**, *222*, 439.
- (14) Pfizer: Product Monograph Neurontin. 2006.
- (15) Backonja, M. M.; Serra, J. *Pain Med.* **2004**, *5* (Suppl 1), S28.
- (16) Taylor, C. P. *Rev. Neurol. (Paris)* **1997**, *153* (Suppl 1), 39.
- (17) Taylor, C. P.; Gee, N. S.; Su, T. Z.; Kocsis, J. D.; Welty, D. F.; Brown, J. P.; Dooley, D. J.; Boden, P.; Singh, L. *Epilepsy Res.* **1998**, *29*, 233.
- (18) Chen, Q.; Richardson, N. V. *Nat. Mater.* **2003**, *2*, 324.
- (19) Kresse, G.; Furthmüller, J. *Comput. Mater. Sci.* **1996**, *6*, 15.
- (20) Kresse, G.; Joubert, D. *Phys. Rev. B* **1999**, *59*, 1758.
- (21) Perdew, J. P.; Chevary, J. A.; Vosko, S. H.; Jackson, K. A.; Pederson, M. R.; Singh, D. J.; Fiolhais, C. *Phys. Rev. B* **1992**, *46*, 6671.
- (22) Ortmann, F.; Bechstedt, F.; Schmidt, W. G. *Phys. Rev. B* **2006**, *73*, 205101.
- (23) Blankenburg, S.; Schmidt, W. G. *Phys. Rev. B* **2006**, *74*, 155419.
- (24) Tabatabaei, J.; Sakakini, B. H.; Watson, M. J.; Waugh, K. C. *Catal. Lett.* **1999**, *59*, 143.
- (25) Genger, T.; Hinrichsen, O.; Muhler, M. *Catal. Lett.* **1999**, *59*, 137.

JP8037297